MANCHESTER 1824
The University of Manchester

The University of Manchester Research

Online Chemical Characterization of Food-Cooking Organic Aerosols

DOI:
10.1021/acs.est.7b06278

Document Version
Accepted author manuscript

Link to publication record in Manchester Research Explorer

Citation for published version (APA):
Reyes-Villegas, E., Bannan, T., Le Breton, M., Mehra, A., Priestley, M., Percival, C., Coe, H., & Allan, J. D. (2018). Online Chemical Characterization of Food-Cooking Organic Aerosols: Implications for Source Apportionment. *Environmental Science and Technology*, *52*(9), 5308-5318. https://doi.org/10.1021/acs.est.7b06278

Published in:
Environmental Science and Technology

Citing this paper
Please note that where the full-text provided on Manchester Research Explorer is the Author Accepted Manuscript or Proof version this may differ from the final Published version. If citing, it is advised that you check and use the publisher's definitive version.

General rights
Copyright and moral rights for the publications made accessible in the Research Explorer are retained by the authors and/or other copyright owners and it is a condition of accessing publications that users recognise and abide by the legal requirements associated with these rights.

Takedown policy
If you believe that this document breaches copyright please refer to the University of Manchester's Takedown Procedures [http://man.ac.uk/04Y6Bo] or contact uml.scholarlycommunications@manchester.ac.uk providing relevant details, so we can investigate your claim.

OPEN ACCESS

Download date:27. Aug. 2022

Online chemical characterization of food cooking organic aerosols: implications for source apportionment

Ernesto Reyes-Villegas[1, *], *Thomas Bannan*[1], *Michael Le Breton*[1, ϕ], *Archit Mehra*[1], *Michael Priestley*[1], *Carl Percival*[1, Δ], *Hugh Coe*[1], *James D. Allan*[1,2, ∇]

[1]School of Earth, Atmospheric and Environmental Sciences, The University of Manchester, Manchester, M13 9PL, UK

[2]National Centre for Atmospheric Science, The University of Manchester, Manchester, M13 9PL, UK

[ϕ]Now at University of Gothenburg, 40530 Gothenburg, Sweden

[Δ]Now at Jet Propulsion Laboratory, 4800 Oak Grove Drive, Pasadena, CA 91109, USA

*Corresponding author: ernesto.reyesvillegas@manchester.ac.uk

Abstract. Food cooking organic aerosols (COA) are one of the main primary sources of submicron particulate matter in urban environments. However, there are still many questions surrounding source apportionment related to instrumentation as well as semi-volatile partitioning as COA evolve rapidly in the ambient air, making source apportionment more complex. Online measurements of emissions from cooking different types of food were performed in a laboratory in order to characterize particles and gases. Aerosol mass spectrometer (AMS) measurements showed that the relative ionization efficiency for OA was higher (1.56 - 3.06) relative to a typical value of 1.4, concluding AMS is overestimating COA and suggesting previous studies likely overestimated COA concentrations. Food cooking mass spectra were generated using AMS and gas and particle food markers were identified with FIGAERO-CIMS measurements to be used in future food cooking source apportionment studies. However, there is a considerable variability both on gas and particle markers and dilution plays an important role in the particle mass budget, showing the importance of using these markers with caution when receptor modeling. These findings can be used to better understand the chemical composition of COA and it provides useful information to be used in future source apportionment studies.

Keywords: AMS, FIGAERO-CIMS, Organic aerosols, Source apportionment, mass spectra.

1. Introduction

Atmospheric aerosols have been found to cause severe air quality problems.[1-3] Food cooking emissions are one of the main indoor and outdoor sources of particles around the world.[4] Cooking Organic Aerosols (COA) represent a high contribution to OA, particularly in urban environments. For instance, Huang, et al. [5], in a study performed during the Olympic Games Beijing 2008, identified that COA contribute 24% while Sun, et al. [6], in a study performed during summer 2009 at Queens College in New York, identified COA to

contribute 16%. Moreover, COA contribution to OA (24%) was found to be higher than traffic-related hydrocarbon-like OA (HOA, 16%) in a study performed in 2012 in Lanzhou China. [7]

In 2005, the first study to identify COA from aerosol mass spectrometer (AMS) measurements was performed by Lanz, et al. [8] in Zurich, Switzerland identifying a 'minor' COA source. Allan, et al. [9] identified, for the first time in the UK, COA, which were found to contribute 34% to OA concentrations. Further ambient OA studies have investigated the COA seasonal trend in the UK[10, 11] and other parts of the world.[12-15] However, follow up studies in Barcelona, Spain did find specific markers for food activities. [16, 17] China, in particular, has performed several studies, over the last decade, towards online chemical aerosol characterization,[18] recognizing cooking emissions to be one of the main primary sources of OA, with studies in urban environments such as Lanzhou,[19, 20] Beijing[21] and Baoji.[22]

While COA have been investigated in different ambient studies, their complexity still makes it challenging to fully characterize their chemical properties. Dall'Osto, et al. [23] performed an in-depth characterization of COA at a rural site, where it was stressed that the COA factor, deconvolved from AMS measurements, included other emissions than food cooking. Another important aspect that makes challenging to quantify COA is the aging occurring in ambient air, making the mass spectra of COA experience a seasonal variation, hence there being a difference in summer and winter.[24]

The use of other techniques to study aerosols allows a better understanding of food cooking aerosols.[4, 18] Receptor modeling is a technique that has been successfully used to perform aerosol source apportionment.[25-27] Multilinear engine (ME-2) is a source apportionment tool that uses information from previous studies (i.e. mass spectra) as inputs to partially constrain

65 solutions when identifying sources.[28] Chemical mass balance (CMB) uses source profiles or
66 fingerprints to identify and quantify source contributions.[29] However, this technique has
67 ambiguities of its own; there are uncertainties related to the representativeness of the profiles
68 used and uncertainties surrounding the effect phenomena such as semi-volatile repartitioning
69 and chemical aging have on the mass budget and markers. This situation increases the
70 complexity to perform COA source apportionment as they evolve rapidly in the ambient air.[23]
71 Over more than 15 years, the Aerodyne aerosol mass spectrometers have proven to be a
72 powerful tool to quantify and characterize the composition of non-refractory submicron
73 aerosol concentrations.[30, 31] However, certain studies have identified an overestimation of OA
74 concentrations measured with AMS when compared to collocated measurements. Yin, et al.
75 [32] found food cooking aerosols, identified with positive matrix factorization (PMF), to
76 overestimate CMB results by a factor of two, in spite of a good correlation. Minguillón, et al.
77 [33] determined organic aerosols-to-organic carbon ratios to be higher than unity, stating this is
78 explained by an underestimation of the relative ion efficiency of OA (RIE_{OA}), a parameter the
79 instrument uses to calculate OA concentrations. Murphy [34] presented a model approach to
80 estimate RIE based on molecular mass. While Jimenez, et al. [35] disagreed that the effect was
81 as strong as suggested, however, both agree that RIE values have the potential to be higher
82 than the typical RIE_{OA}=1.4.[36]
83 There has been a wide range of controlled experiments to investigate different aspects of
84 food cooking aerosols. [37-39] However, until now there has been no laboratory study analyzing
85 both particle and gas phase emissions using online measurements. Here, we present combined
86 on-line measurements of the high-resolution time-of-flight aerosol mass spectrometer (HR-
87 ToF-AMS) and the filter inlet for gases and aerosols (FIGAERO) attached to the high-
88 resolution time-of-flight chemical ionization mass spectrometer (HR-ToF-CIMS). The HR-
89 ToF-AMS quantifies high time resolution concentrations of OA. However, there is no

molecular information due to the ion fragmentation produced by the strong electron ionization. Hence, the characterization of particles collected with FIGAERO and together with the soft chemical ionization from HR-ToF-CIMS provides additional information such as molecular weight and chemical formula of species within both the gas and particle phases, which will help in bridging the gap between PMF-AMS and CMB analyses and also to assist in interpreting ambient FIGAERO-CIMS data.

This study aims to provide a better understanding of food cooking aerosol chemical characterization, focusing on three main scientific objectives: 1. To investigate potential AMS quantification issues regarding COA; 2. To provide profiles in both the AMS and CIMS to assist in the interpretation of field data; 3. To establish whether emissions from cooking are semi-volatile, and to what extent this may impact upon source apportionment techniques.

2. Methodology

2.1 Measurements. Online measurements of gases and particles, emitted from cooking different types of food, were carried out in a laboratory. A variety of food (fish and chips, English breakfast, vegetables and different types of meat) was cooked using rapeseed (canola) oil. Two types of electric cooking equipment were used; a deep fryer, using three liters of cooking oil; and an induction hob to shallow fry in a pan with a diameter of 22 cm. When shallow frying meat on a flat frying pan, two cooking styles were used; stir-fried, which involves chopping meat into small pieces and stirring meat while cooking; and chop frying. The different cooking methods were used to determine whether they would have an effect on the aerosol chemical composition. The cooking time of each food was between 4-8 minutes depending on the time needed for the food to be completely cooked. A total of 36 experiments were performed. Emissions were directed to a movable extraction cowling where the common sample inlet was located (Figure S1). The sample inlet was optionally attached

115 to a diluter (Dekati, DI-100), using compressed air to obtain a dilution factor of
116 approximately 1:10. Diluted/non-diluted experiments were performed to investigate gas semi-
117 volatile behavior and its effect on the aerosol budget.

118 2.2 HR-ToF-AMS and SMPS measurements. Submicron non-refractory aerosol
119 concentrations (OA, SO_4^{2-}, NH_4^+, NO_3^-, and Cl^-) were measured with a HR-ToF-AMS [31],
120 hereafter AMS. The procedure to quantify AMS mass concentrations has been previously
121 described [40, 41]. The two main parameters AMS uses to quantify aerosol concentrations are
122 collection efficiency (CE) and relative ionization efficiency (RIE). The CE measures how
123 well particles are transmitted and detected, depending on three terms: the transmission
124 efficiency of the aerodynamic lenses, the transmission loss due to nonsphericity of particles
125 and bouncing of particles when impacting the vaporizer [42, 43]. Aerosols that tend to be liquid
126 and with diameters between 60 and 600 nanometers (nm) present high CE [44, 45], thus in this
127 study, a CE = 1.0 was used. RIE is the ratio of IE of a given analyte (defined as ions detected
128 per available vapor molecule) relative to the IE of nitrate obtained from ammonium nitrate
129 calibrations. The default value of RIE for OA (RIE_{OA}=1.4) used. [35, 36] However, after
130 comparing the AMS aerosol concentrations with Scanning Mobility Particle Sizer (SMPS)
131 measurements, it was found AMS to overestimate aerosol concentrations. This
132 overestimation is attributed to RIE_{OA} to be higher than 1.4. Further details are provided in
133 the Supplement S1. Elemental analysis was performed as described by Aiken, et al. [46] with
134 the "improved ambient" method proposed by Canagaratna, et al. [47].

135 Particle number concentration and size distribution, with mobility diameter ranging from
136 18 to 514 nm, were measured using an SMPS (model 3936, TSI). In order to compare SMPS
137 with AMS measurements, a density of 0.85 $g \cdot cm^{-3}$, average density of rapeseed oil and oleic
138 acid [48], was used to convert SMPS volume concentration to mass concentration.

2.3 FIGAERO-HR-ToF-CIMS measurements. The HR-ToF-CIMS, hereafter CIMS, with iodide (I^-) as reagent ion [49], was used to measure oxidized organic compounds in the gas phase. [50] FIGAERO, coupled to the CIMS measured particle composition. CIMS measured gases over the time food was being cooked while particles were collected on a filter in the FIGAERO inlet. The gas phase measurements were followed by desorption of the collected particles into the CIMS, using a programmed desorption step, where 2 slpm flow of N_2 was ramped from ambient temperature up to 200° C over 15 minutes and passed through the filter into the inlet to be detected by the CIMS. Both gases and particles were collected using a flow of 2 slpm. Aerosols emitted when cooking English breakfast (composed of tomato, mushroom, eggs, bacon, black pudding and sausages) were collected on one filter, other experiments were also collected in one filter when cooking the same type of food, for example, stir-fried chicken and chop fried chicken. Table 1 shows the desorbed filters using this procedure. Details about FIGAERO-CIMS calibration is provided in Supplement S2.

3 Results

3.1 Aerosol concentrations overview. A wide range of aerosol concentrations was measured with AMS and SMPS. Table 1 shows the information for the performed experiments; non-diluted and diluted, using deep fried and shallow fried as cooking methods. Looking at SMPS concentrations of non-diluted experiments, higher aerosol concentrations were present on shallow fried compared to deep frying. For shallow fried experiments, aerosol average concentrations range from 9.6 $\mu g \cdot m^{-3}$ for black pudding to 395 $\mu g \cdot m^{-3}$ for sausages, while deep frying concentrations ranged between 4.3 – 223.5 $\mu g \cdot m^{-3}$. Other high concentrations include tomato (226.5 $\mu g \cdot m^{-3}$) and bacon (247.6 $\mu g \cdot m^{-3}$). The fact that tomato shows high concentrations may be explained by the fact that tomato was chopped in half and there was more surface area in contact with the oil/pan. Moreover, the chopped tomato would have a high moisture content, causing more sizzling and therefore mechanical ejection.

3.2 AMS oxidation state. Elemental analysis (oxygen and hydrogen to carbon ratios, O:C and H:C) is an approach to explore the oxidation state of OA. In this study O:C and H:C mean and standard deviation ellipse (SDE) were calculated for the experiments matching with the filters collected with FIGAERO (F0-F17), to study the OA oxidation state which may have implications on source apportionment. The standard deviation ellipse (SDE) used in the graphs to denote spread was calculated following the equations detailed in Gong [51]. Figure 1 shows the Van Krevelen diagram with O:C and H:C ratios. When analyzing the SDE in Figure 1.b, shallow frying (continuous lines) shows the greater variability both in O:C and H:C ratios compared to deep frying and (dotted lines). The variation in ratios when shallow frying is expected as this type of cooking involves flipping over the meat and/or stirring food while deep frying cooks food with continuous heating of three litters of oil and relatively little disturbance of the food itself. These findings suggest the effect cooking styles may have on aerosol composition.

Diluted experiments showed higher mean O:C ratios compared to non-diluted experiments (Fig. 1.d): English breakfast, deep fried sausages and Deep fried burgers with 0.28 (F11), 0.28 (F9) and 0.25 (F3) for diluted compared to 0.23 (F10), 0.17 (F8) and 0.19 (F8) for not diluted, respectively. This increment on O:C may result from the evaporation of more volatile molecules, leaving a relatively larger fraction of less volatile molecules with a possible higher O:C in the particle phase.

Circles and dotted lines represent deep frying samples in 1.a and 1.b and non-diluted samples in 1.c and 1.d. Triangles and continuous lines represent shallow frying samples in 1.a and 1.b and diluted samples in 1.c and 1.d. OS represents the oxidation state which increases with oxidative aging.[52] Blue and red dotted lines in 1.a represent f44 and f43 as used on the triangle plot proposed by Ng, et al. [53]. Figures 1.b and 1.d are a zoomed version of figures 1.a and 1.c respectively. Description of filters (f0-f17) is provided in Table 1.

Mean O:C (0.15-0.32) and H:C (1.69-1.86) values observed in this study are compared to the ones seen in the literature. Kaltsonoudis, et al. [24] in a laboratory study from charbroiling meat, exposing emissions to UV illumination and oxidants, found O:C values of 0.09-0.3, with O:C ratios increasing with chemical aging. Ambient O:C ratios from COA have been found with values of (0.10- 0.22). [7, 47, 54, 55] These values are similar to other POA such as HOA with values of 0.14-0.38 [47, 54, 56, 57], though HOA presents a higher H:C ratio. While high O:C ratios have been seen on secondary OA (SOA) 0.52-1.02. [47, 54, 56] This increment in O:C ratios from POA to SOA is due to the chemical aging aerosols present in the atmosphere.

While O:C and H:C ratios of this study are similar compared to the ratios from food cooking aerosols found in the literature, O:C and H:C ratios from food cooking aerosols are different from the ones of other primary OA such as HOA, which has a higher H:C or secondary OA with a higher O:C (Refer to Table S4 for more O:C ratios from literature). Diluted experiments presented an increment on O:C, showing what would be expected to happen when aerosols are emitted to the atmosphere with further dilution and aging, as we qualitatively expect the more polar compounds to have a lower vapor pressure.[58] Laboratory studies aiming to determine food cooking markers should consider performing diluted experiments to better represent ambient conditions.

3.3 FIGAERO - AMS comparison. The soft chemical ionization of the CIMS provides molecular information of chemical species and, with the use of the FIGAERO inlet, it is possible to identify food cooking markers both in particle and gas phase. In this study, 128 compounds were identified in the gas phase, from which 69 were also identified in the particle phase (Table S3). The sum of the average concentration of the 69 compounds in particle phase, identified in each desorbed filter, was compared to the average OA measurements from AMS. This comparison was performed as a way to validate particle measurements obtained from the FIGAERO. Table 1 indicates the filters taken with

214 FIGAERO to which AMS averages were calculated. Due to a technical issue, no filter data is
215 available for the first six filters (F0 to F5), thus the following FIGAERO-CIMS analysis will
216 be performed from filters F6 to F17. Additionally, a comparison was performed using
217 levoglucosan, which is a compound identified both with FIGAERO-CIMS and AMS
218 instruments. In the AMS it is typically identified at m/z 60 [59] while in the FIGAERO-CIMS it
219 is identified with molecular mass 288.96 g.mol^{-1} (molecular mass of $C_6H_{10}O_5$ + I). Figure 2
220 shows non-diluted deep fried sausages (F9) and English breakfast (F10) are the experiments
221 with the highest aerosol concentrations. Both levoglucosan (Figure 2.a) and total aerosol
222 concentrations (Figure2.b) present similar trend. A strong correlation is observed with r =
223 0.88 for the levoglucosan comparison and r = 0.83 for the total particles comparison.
224 FIGAERO measured 22 times higher levoglucosan concentrations, which is expected as
225 AMS concentrations are the m/z 60 related, a fragment related to levoglucosan. While in the
226 total aerosol comparison, FIGAERO quantified 80% of OA measured by the AMS, results
227 consistent with previous studies, which have identified FIGAERO to quantify 25-50% of OA
228 concentrations. [60-62]

229 **3.4 FIGAERO-CIMS food cooking markers**

230 Deep frying emitted more gases than shallow frying (Table 2), which is expected due to the
231 larger amount of oil used during deep frying. Eight organic acids were identified as cooking
232 markers in the gas phase: isocyanic (HNCO), formic (CH_2O_2), acrylic ($C_3H_4O_2$), propionic
233 ($C_3H_6O_2$), hydroxypropionic ($C_3H_6O_3$), malonic ($C_3H_4O_4$), hexanoic ($C_6H_{12}O_2$) and adipic
234 ($C_6H_{10}O_4$). These organic acids were chosen as markers as they were present in all cooking
235 samples with high concentrations. Hydroxypropionic acid was the compound with a higher
236 presence in gas phase both on deep frying and shallow frying. In general, HNCO
237 concentrations were identified in the majority of the samples. HNCO has been related to
238 biomass burning [63] and traffic emissions.[64] However, to our knowledge, no studies in the

239 literature have reported HNCO concentrations emitted from food cooking. Roberts, et al. [65]
240 reported HNCO concentrations to be related to coal used as a fuel to cook but not to the food
241 itself.

242 Nitrogen-containing compounds have been previously found to have negative effects to
243 human health [66] and have been identified on cooking emissions. [4] They may be emitted either
244 from the food itself or also from additives. In this study, 14 different nitrogen-containing
245 compounds were identified both in the gas and particle phase (Table S5). $C_4H_2NO_2$ and
246 parabanic acid ($C_3H_2N_2O_3$), during deep-frying experiments, were identified only in the gas
247 phase. The rest of the nitrogen-containing compounds were identified mainly in the particle
248 phase: Creatinine ($C_4H_7N_3O$), nitrobenzene ($C_6H_5NO_2$), $C_6H_7NO_2$, $C_5H_7N_2O_2$, $C_5H_8NO_3$,
249 $C_6H_{13}NO_2$, $C_5H_9N_3O_2$ and $C_{13}H_{15}NO_2$ were present only in shallow frying experiments.
250 Nicotinamide ($C_6H_6N_2O$), nitrobenzene, $C_6H_7NO_2$ and $C_5H_8NO_3$ were mainly emitted from
251 non-diluted deep fried sausages (filter9), diluted shallow fried pork (filter15) and diluted
252 shallow fried lamb (filter16). While it was not possible to determine or speculate at the
253 structure of many of the identified nitrogen-containing compounds, given the potential
254 impacts of this compound class, it is worth reporting their presence and contribution to food
255 cooking emissions, which were mainly found in the particle phase. Further studies should be
256 aimed to further characterize and quantify these nitrogen-containing compounds.

257 **4 Discussion**

258 **4.1 Relative Ion Efficiency of OA.** The AMS has been widely used to measure the
259 chemical composition of non-refractory aerosols. However, it has been found to report food
260 cooking OA concentrations to be greater than other measurement techniques.[32] Table S1
261 shows OA has higher concentrations compared to SMPS, resulting in OA/SMPS ratios to be
262 higher than unity. OA concentrations were originally calculated with RIE_{OA}= 1.4. as
263 suggested by Alfarra, et al. [36]. However, it has been previously shown that RIE_{OA} values may

264 vary within functional groups.[40] An increment on RIE_{OA} will decrease the reported OA
265 concentration. Hence, the hypothesis here is that the overestimation of OA measurements
266 compared to SMPS is due to RIE_{OA} to be higher than 1.4.

267 This shows that RIE_{OA_corr} values are higher than 1.4, with values between 1.56 and 3.06
268 (Table S2). The highest RIE_{OA_corr} value of 3.06 was observed with diluted deep fried
269 experiments. This value is in agreement with Murphy [34] and Jimenez, et al. [35], who reported
270 oleic acid to have an RIE of 2.8-4.0 and 3.2 respectively. After heating, oleic acid is the main
271 component of rapeseed oil 63% - 70% [67, 68], and this hypothesis is further supported by the
272 fact that high RIE_{OA_corr} values were present with deep fried experiments, where much of the
273 particulate matter likely originates from the recondensation of semivolatiles from the oil or
274 the mechanical ejection of oil by bubbles bursting during frying. The low RIE_{OA_corr} values
275 for shallow fried indicate that the OA emissions from meat and vegetables have RIEs closer
276 to the default of 1.4.

277 The increment on RIE_{OA}, combined with the assumed CE of 1, found in this study explains
278 the good correlation but quantitative disagreement between PMF-AMS and CMB reported by
279 Yin, et al. [32] and also agrees with Minguillón, et al. [33] who also found RIE_{OA} to be higher than
280 1.4. It is worth mentioning a possible limitation of SMPS mass concentrations obtained is that
281 a density of 0.85 $g \cdot cm^{-3}$ is assumed, which may not be accurate. However, the deviations in
282 RIE reported are deemed to be larger than the plausible uncertainty in density. The RIE result
283 has significant implications for ambient measurements of COA. While COA concentrations
284 have often been reported to be a significant contribution to primary OA aerosol
285 concentrations, these could have been overestimated in previous studies. However, it is
286 unlikely that the bulk OA concentrations have been systematically misreported overall, as
287 these have frequently compared favorably with external comparisons.[35] If the COA

288 specifically is being over-reported, then this should be accordingly corrected after it has been
289 isolated using factorization.

290 **4.2 Food cooking AMS mass spectra.** Source apportionment tools, like the multilinear
291 engine (ME-2), use inputs in the way of mass spectra or time series, to partially constrain
292 solutions and better deconvolve OA sources.[28] Mass spectra of COA have certain
293 characteristics that make them different to mass spectra from other sources, for example the
294 signals at m/z 41, m/z 55 and m/z 57, with a higher signal at m/z 55 compared to m/z 57. [9, 12,
295 23] The generation of mass spectra, from different types of food cooking and a better
296 understanding of their variations, will help to improve COA source apportionment. In this
297 study, a comparison was performed within the mass spectra obtained from the experiments
298 and with the mass spectra from other ambient and laboratory studies. Table S6 shows the
299 uncentered Pearson's correlation coefficients ($_{u}r$, also known as the 'normalized dot product'
300 or 'cosine angle') and Table S7 shows the list of external mass spectra used in the
301 comparison.

302 The correlations performed within the experiments showed high $_{u}r$ values ranging from
303 0.876 when comparing two different cooking and meat types (diluted shallow fried chicken
304 vs non-diluted deep fried burgers) to 0.999 when comparing deep fried burgers diluted vs
305 non-diluted. Fish and chips and English breakfast also showed high $_{u}r$ values when
306 comparing diluted and non-diluted experiments, suggesting diluting presents little effect on
307 mass spectra.

308 A decrease on correlations were observed when comparing the mass spectra of this study
309 with COA mass spectra from previous ambient studies, with $_{u}r$ values from 0.734 (non-
310 diluted deep fried fish and chips vs COA from Lanz, et al. [8]) to 0.991 (diluted deep fried
311 sausages vs COA from Reyes-Villegas, et al. [69]). The low correlations obtained when
312 comparing mass spectra of this study with COA from Lanz, et al. [8] might be expected as the

later was the first PMF-AMS study, focused more on the development of the methodology and was contained within a higher-order solution, where the authors expressed doubts as to its accuracy.

From these correlations, we can see that when cooking different types of meat/vegetables and using a variety of cooking styles (deep frying and shallow frying), mass spectra from fresh emissions do not vary significantly. However, the decrease in $_{u}r$ values when compared with mass spectra from past ambient studies from the literature, suggests aging of food cooking aerosols (through repartitioning or chemical reactions) in the atmosphere that are not capture here.

4.3 Effect of dilution on food cooking aerosols. From the desorption analysis, 69 compounds were identified in the particle phase (Table S3). From this list, Table 4 shows the 12 compounds that have been previously identified as cooking markers [4, 26, 70, 71] Levoglucosan ($C_6H_{10}O_5$), dicarboxylic acids: succinic ($C_4H_6O_4$), glutaric ($C_5H_8O_4$), pimelic ($C_7H_{12}O_4$), suberic ($C_8H_{14}O_4$), azelaic ($C_9H_{16}O_4$), sebacic ($C_{10}H_{18}O_4$), dodecanedioic ($C_{12}H_{22}O_4$), and carboxylic acids: palmitic ($C_{16}H_{32}O_2$), margaric ($C_{17}H_{34}O_2$), linoleic ($C_{18}H_{32}O_2$) and oleic ($C_{18}H_{34}O_2$). However, the majority of these markers have been identified from off-line measurements or from gas and particle measurements in separate studies. Here we show near real-time measurements of both gases and particles, gas-to-particle ratios (G/P) and the effect of dilution.

These 12 compounds are considered to be cooking markers in the particle phase as they were found mainly during the filter desorption. Even when they were identified as being present in the gas phase, the G/P ratio is still lower than unity. In contrast, for the gas phase cooking markers presented in Table 2, the G/P ratio was greater than unity. G/P ratios were calculated from average gas and particle counts·sec^{-1} (Table 3). It is worth mentioning that some of these compounds are also found to be in other sources; for example, levoglucosan

has been used as a marker of biomass burning aerosols.[70] Succinic, glutaric, pimelic acids and levoglucosan were found mainly in the gas phase for the diluted deep frying experiments (F7 and F8). Denoting the high variability of gas-particle partitioning and the implication of different cooking conditions in the food cooking emissions.

Higher G/P ratios were observed with diluted experiments compared to non-diluted. Deep fried sausages (F9) present higher G/P ratios with Succinic, glutaric, pimelic, levoglucosan, suberic and azealic compared with diluted deep fried sausages (F8). A similar situation was present with diluted and non-diluted deep fried burgers (F7 and F6 respectively) and English breakfast (F11 and F10 respectively). This behavior is explained in that with diluting experiments, light molecular masses will tend to be more in the gas phase than species with high molecular mass, which will tend to stay in the particle phase. This suggests that the use of these as cooking markers for CMB analysis may be problematic, as their particle-phase concentrations may diminish with dilution, although whether this creates a positive or negative artifact will depend on whether their rate of evaporation is consistent with that of the overall mass of particulate used in the mass balance model.

ASSOCIATED CONTENT

Supporting Information

The supplement material includes a figure showing the instrument arrangement (Figure S1), a list of all cooking experiments (Table S1), a table with AMS and SMPS average concentrations (Table S2), a figure with mass and number size distributions (Figure S2), a list of all the compounds identified on gas and particle (Table S3), a table with O:C and H:C ratios from the literature (Table S4), a table with nitrogen-containing markers (Table S5), a table with uncentered Pearson values for mass spectra comparison (Table S6) and a list with the references of the external cooking mass spectra used on the comparison (Table S7).

AUTHOR INFORMATION

Corresponding author.

* e-mail: ernesto.reyesvillegas@manchester.ac.uk

∇ e-mail: james.allan@manchester.ac.uk

Notes

The authors declare no competing financial interest.

ACKNOWLEDGMENTS

Ernesto Reyes-Villegas is supported by a studentship by the National Council of Science and Technology-Mexico (CONACYT) under registry number 217687.

REFERENCES

(1) Pope III, C. A.; Dockery, D. W., Health effects of fine particulate air pollution: lines that connect. *J Air Waste Manage* **2006,** *56*, (6), 709-742.

(2) Fuzzi, S.; Baltensperger, U.; Carslaw, K.; Decesari, S.; Denier van der Gon, H.; Facchini, M. C.; Fowler, D.; Koren, I.; Langford, B.; Lohmann, U.; Nemitz, E.; Pandis, S.; Riipinen, I.; Rudich, Y.; Schaap, M.; Slowik, J. G.; Spracklen, D. V.; Vignati, E.; Wild, M.; Williams, M.; Gilardoni, S., Particulate matter, air quality and climate: lessons learned and future needs. *Atmos. Chem. Phys.* **2015,** *15*, (14), 8217-8299.

(3) Samoli, E.; Atkinson, R. W.; Analitis, A.; Fuller, G. W.; Beddows, D.; Green, D. C.; Mudway, I. S.; Harrison, R. M.; Anderson, H. R.; Kelly, F. J., Differential health effects of short-term exposure to source-specific particles in London, U.K. *Environ Int* **2016,** *97*, (Supplement C), 246-253.

(4) Abdullahi, K. L.; Delgado-Saborit, J. M.; Harrison, R. M., Emissions and indoor concentrations of particulate matter and its specific chemical components from cooking: A review. *Atmos Environ* **2013,** *71*, 260-294.

(5) Huang, X. F.; He, L. Y.; Hu, M.; Canagaratna, M. R.; Sun, Y.; Zhang, Q.; Zhu, T.; Xue, L.; Zeng, L. W.; Liu, X. G.; Zhang, Y. H.; Jayne, J. T.; Ng, N. L.; Worsnop, D. R., Highly time-resolved chemical characterization of atmospheric submicron particles during 2008 Beijing Olympic Games using an Aerodyne High-Resolution Aerosol Mass Spectrometer. *Atmos Chem Phys* **2010,** *10*, (18), 8933-8945.

(6) Sun, Y. L.; Zhang, Q.; Schwab, J. J.; Demerjian, K. L.; Chen, W. N.; Bae, M. S.; Hung, H. M.; Hogrefe, O.; Frank, B.; Rattigan, O. V.; Lin, Y. C., Characterization of the sources and processes of organic and inorganic aerosols in New York city with a high-resolution time-of-flight aerosol mass apectrometer. *Atmos Chem Phys* **2011,** *11*, (4), 1581-1602.

(7) Xu, J.; Zhang, Q.; Chen, M.; Ge, X.; Ren, J.; Qin, D., Chemical composition, sources, and processes of urban aerosols during summertime in northwest China: insights from high-resolution aerosol mass spectrometry. *Atmos. Chem. Phys.* **2014,** *14*, (23), 12593-12611.
(8) Lanz, V. A.; Alfarra, M. R.; Baltensperger, U.; Buchmann, B.; Hueglin, C.; Prevot, A. S. H., Source apportionment of submicron organic aerosols at an urban site by factor analytical modelling of aerosol mass spectra. *Atmos Chem Phys* **2007,** *7*, (6), 1503-1522.
(9) Allan, J. D.; Williams, P. I.; Morgan, W. T.; Martin, C. L.; Flynn, M. J.; Lee, J.; Nemitz, E.; Phillips, G. J.; Gallagher, M. W.; Coe, H., Contributions from transport, solid fuel burning and cooking to primary organic aerosols in two UK cities. *Atmos Chem Phys* **2010,** *10*, (2), 647-668.
(10) Young, D. E.; Allan, J. D.; Williams, P. I.; Green, D. C.; Flynn, M. J.; Harrison, R. M.; Yin, J.; Gallagher, M. W.; Coe, H., Investigating the annual behaviour of submicron secondary inorganic and organic aerosols in London. *Atmos. Chem. Phys.* **2015,** *15*, (11), 6351-6366.
(11) Reyes-Villegas, E.; Green, D. C.; Priestman, M.; Canonaco, F.; Coe, H.; Prévôt, A. S. H.; Allan, J. D., Organic aerosol source apportionment in London 2013 with ME-2: exploring the solution space with annual and seasonal analysis. *Atmos. Chem. Phys.* **2016,** *16*, (24), 15545-15559.
(12) Mohr, C.; DeCarlo, P. F.; Heringa, M. F.; Chirico, R.; Slowik, J. G.; Richter, R.; Reche, C.; Alastuey, A.; Querol, X.; Seco, R.; Penuelas, J.; Jimenez, J. L.; Crippa, M.; Zimmermann, R.; Baltensperger, U.; Prevot, A. S. H., Identification and quantification of organic aerosol from cooking and other sources in Barcelona using aerosol mass spectrometer data. *Atmos Chem Phys* **2012,** *12*, (4), 1649-1665.
(13) Crippa, M.; Canonaco, F.; Lanz, V. A.; Aijala, M.; Allan, J. D.; Carbone, S.; Capes, G.; Ceburnis, D.; Dall'Osto, M.; Day, D. A.; DeCarlo, P. F.; Ehn, M.; Eriksson, A.; Freney, E.; Ruiz, L. H.; Hillamo, R.; Jimenez, J. L.; Junninen, H.; Kiendler-Scharr, A.; Kortelainen, A. M.; Kulmala, M.; Laaksonen, A.; Mensah, A.; Mohr, C.; Nemitz, E.; O'Dowd, C.; Ovadnevaite, J.; Pandis, S. N.; Petaja, T.; Poulain, L.; Saarikoski, S.; Sellegri, K.; Swietlicki, E.; Tiitta, P.; Worsnop, D. R.; Baltensperger, U.; Prevot, A. S. H., Organic aerosol components derived from 25 AMS data sets across Europe using a consistent ME-2 based source apportionment approach. *Atmos Chem Phys* **2014,** *14*, (12), 6159-6176.
(14) Frohlich, R.; Crenn, V.; Setyan, A.; Belis, C. A.; Canonaco, F.; Favez, O.; Riffault, V.; Slowik, J. G.; Aas, W.; Aijala, M.; Alastuey, A.; Artinano, B.; Bonnaire, N.; Bozzetti, C.; Bressi, M.; Carbone, C.; Coz, E.; Croteau, P. L.; Cubison, M. J.; Esser-Gietl, J. K.; Green, D. C.; Gros, V.; Heikkinen, L.; Herrmann, H.; Jayne, J. T.; Lunder, C. R.; Minguillon, M. C.; Mocnik, G.; O'Dowd, C. D.; Ovadnevaite, J.; Petralia, E.; Poulain, L.; Priestman, M.; Ripoll, A.; Sarda-Esteve, R.; Wiedensohler, A.; Baltensperger, U.; Sciare, J.; Prevot, A. S. H., ACTRIS ACSM intercomparison - Part 2: Intercomparison of ME-2 organic source apportionment results from 15 individual, co-located aerosol mass spectrometers. *Atmos Meas Tech* **2015,** *8*, (6), 2555-2576.
(15) Bozzetti, C.; El Haddad, I.; Salameh, D.; Daellenbach, K. R.; Fermo, P.; Gonzalez, R.; Minguillon, M. C.; Iinuma, Y.; Poulain, L.; Elser, M.; Muller, E.; Slowik, J. G.; Jaffrezo, J. L.; Baltensperger, U.; Marchand, N.; Prevot, A. S. H., Organic aerosol source apportionment by offline-AMS over a full year in Marseille. *Atmos Chem Phys* **2017,** *17*, (13), 8247-8268.
(16) Alier, M.; van Drooge, B. L.; Dall'Osto, M.; Querol, X.; Grimalt, J. O.; Tauler, R., Source apportionment of submicron organic aerosol at an urban background and a road site in Barcelona (Spain) during SAPUSS. *Atmos. Chem. Phys.* **2013,** *13*, (20), 10353-10371.
(17) Dall'Osto, M.; Beddows, D. C. S.; McGillicuddy, E. J.; Esser-Gietl, J. K.; Harrison, R. M.; Wenger, J. C., On the simultaneous deployment of two single-particle mass spectrometers at an urban background and a roadside site during SAPUSS. *Atmos. Chem. Phys.* **2016,** *16*, (15), 9693-9710.
(18) Li, Y. J.; Sun, Y.; Zhang, Q.; Li, X.; Li, M.; Zhou, Z.; Chan, C. K., Real-time chemical characterization of atmospheric particulate matter in China: A review. *Atmos Environ* **2017,** *158*, 270-304.
(19) Zhang, X.; Zhang, Y.; Sun, J.; Yu, Y.; Canonaco, F.; Prévôt, A. S. H.; Li, G., Chemical characterization of submicron aerosol particles during wintertime in a northwest city of China using an Aerodyne aerosol mass spectrometry. *Environmental Pollution* **2017,** *222*, (Supplement C), 567-582.

(20) Xu, J. Z.; Shi, J. S.; Zhang, Q.; Ge, X. L.; Canonaco, F.; Prevot, A. S. H.; Vonwiller, M.; Szidat, S.; Ge, J. M.; Ma, J. M.; An, Y. Q.; Kang, S. C.; Qin, D. H., Wintertime organic and inorganic aerosols in Lanzhou, China: sources, processes, and comparison with the results during summer. *Atmos Chem Phys* **2016,** *16*, (23), 14937-14957.
(21) Bei, N.; Wu, J.; Elser, M.; Feng, T.; Cao, J.; El-Haddad, I.; Li, X.; Huang, R.; Li, Z.; Long, X.; Xing, L.; Zhao, S.; Tie, X.; Prévôt, A. S. H.; Li, G., Impacts of meteorological uncertainties on the haze formation in Beijing–Tianjin–Hebei (BTH) during wintertime: a case study. *Atmos. Chem. Phys.* **2017,** *17*, (23), 14579-14591.
(22) Wang, Y. C.; Huang, R. J.; Ni, H. Y.; Chen, Y.; Wang, Q. Y.; Li, G. H.; Tie, X. X.; Shen, Z. X.; Huang, Y.; Liu, S. X.; Dong, W. M.; Xue, P.; Fröhlich, R.; Canonaco, F.; Elser, M.; Daellenbach, K. R.; Bozzetti, C.; El Haddad, I.; Prévôt, A. S. H.; Canagaratna, M. R.; Worsnop, D. R.; Cao, J. J., Chemical composition, sources and secondary processes of aerosols in Baoji city of northwest China. *Atmos Environ* **2017,** *158*, 128-137.
(23) Dall'Osto, M.; Paglione, M.; Decesari, S.; Facchini, M. C.; O'Dowd, C.; Plass-Duellmer, C.; Harrison, R. M., On the Origin of AMS "Cooking Organic Aerosol" at a Rural Site. *Environmental Science & Technology* **2015,** *49*, (24), 13964-13972.
(24) Kaltsonoudis, C.; Kostenidou, E.; Louvaris, E.; Psichoudaki, M.; Tsiligiannis, E.; Florou, K.; Liangou, A.; Pandis, S. N., Characterization of fresh and aged organic aerosol emissions from meat charbroiling. *Atmos. Chem. Phys.* **2017,** *17*, (11), 7143-7155.
(25) Zhang, Q.; Jimenez, J. L.; Canagaratna, M. R.; Ulbrich, I. M.; Ng, N. L.; Worsnop, D. R.; Sun, Y., Understanding atmospheric organic aerosols via factor analysis of aerosol mass spectrometry: a review. *Analytical and bioanalytical chemistry* **2011,** *401*, (10), 3045-3067.
(26) Mancilla, Y.; Mendoza, A.; Fraser, M. P.; Herckes, P., Organic composition and source apportionment of fine aerosol at Monterrey, Mexico, based on organic markers. *Atmos. Chem. Phys.* **2016,** *16*, (2), 953-970.
(27) Hopke, P. K., Review of receptor modeling methods for source apportionment. *J Air Waste Manage* **2016,** *66*, (3), 237-259.
(28) Canonaco, F.; Crippa, M.; Slowik, J. G.; Baltensperger, U.; Prevot, A. S. H., SoFi, an IGOR-based interface for the efficient use of the generalized multilinear engine (ME-2) for the source apportionment: ME-2 application to aerosol mass spectrometer data. *Atmos Meas Tech* **2013,** *6*, (12), 3649-3661.
(29) Mugica, V.; Vega, E.; Chow, J.; Reyes, E.; Sánchez, G.; Arriaga, J.; Egami, R.; Watson, J., Speciated non-methane organic compounds emissions from food cooking in Mexico. *Atmos Environ* **2001,** *35*, (10), 1729-1734.
(30) Jayne, J. T.; Leard, D. C.; Zhang, X. F.; Davidovits, P.; Smith, K. A.; Kolb, C. E.; Worsnop, D. R., Development of an aerosol mass spectrometer for size and composition analysis of submicron particles. *Aerosol Science and Technology* **2000,** *33*, (1-2), 49-70.
(31) DeCarlo, P. F.; Kimmel, J. R.; Trimborn, A.; Northway, M. J.; Jayne, J. T.; Aiken, A. C.; Gonin, M.; Fuhrer, K.; Horvath, T.; Docherty, K. S.; Worsnop, D. R.; Jimenez, J. L., Field-deployable, high-resolution, time-of-flight aerosol mass spectrometer. *Anal Chem* **2006,** *78*, (24), 8281-8289.
(32) Yin, J.; Cumberland, S. A.; Harrison, R. M.; Allan, J.; Young, D. E.; Williams, P. I.; Coe, H., Receptor modelling of fine particles in southern England using CMB including comparison with AMS-PMF factors. *Atmos. Chem. Phys.* **2015,** *15*, (4), 2139-2158.
(33) Minguillón, M. C.; Ripoll, A.; Pérez, N.; Prévôt, A. S. H.; Canonaco, F.; Querol, X.; Alastuey, A., Chemical characterization of submicron regional background aerosols in the western Mediterranean using an Aerosol Chemical Speciation Monitor. *Atmos. Chem. Phys.* **2015,** *15*, (11), 6379-6391.
(34) Murphy, D. M., The effects of molecular weight and thermal decomposition on the sensitivity of a thermal desorption aerosol mass spectrometer. *Aerosol Science and Technology* **2016,** *50*, (2), 118-125.
(35) Jimenez, J. L.; Canagaratna, M. R.; Drewnick, F.; Allan, J. D.; Alfarra, M. R.; Middlebrook, A. M.; Slowik, J. G.; Zhang, Q.; Coe, H.; Jayne, J. T.; Worsnop, D. R., Comment on "The effects of molecular

494 weight and thermal decomposition on the sensitivity of a thermal desorption aerosol mass
495 spectrometer". *Aerosol Science and Technology* **2016,** *50*, (9), i-xv.
496 (36) Alfarra, M. R.; Coe, H.; Allan, J. D.; Bower, K. N.; Boudries, H.; Canagaratna, M. R.; Jimenez, J. L.;
497 Jayne, J. T.; Garforth, A. A.; Li, S.-M.; Worsnop, D. R., Characterization of urban and rural organic
498 particulate in the Lower Fraser Valley using two Aerodyne Aerosol Mass Spectrometers. *Atmos*
499 *Environ* **2004,** *38*, (34), 5745-5758.
500 (37) Mohr, C.; Huffman, J. A.; Cubison, M. J.; Aiken, A. C.; Docherty, K. S.; Kimmel, J. R.; Ulbrich, I. M.;
501 Hannigan, M.; Jimenez, J. L., Characterization of Primary Organic Aerosol Emissions from Meat
502 Cooking, Trash Burning, and Motor Vehicles with High-Resolution Aerosol Mass Spectrometry and
503 Comparison with Ambient and Chamber Observations. *Environmental Science & Technology* **2009,**
504 *43*, (7), 2443-2449.
505 (38) Zhao, X. Y.; Hu, Q. H.; Wang, X. M.; Ding, X.; He, Q. F.; Zhang, Z.; Shen, R. Q.; Lu, S. J.; Liu, T. Y.;
506 Fu, X. X.; Chen, L. G., Composition profiles of organic aerosols from Chinese residential cooking: case
507 study in urban Guangzhou, south China. *J Atmos Chem* **2015,** *72*, (1), 1-18.
508 (39) Amouei Torkmahalleh, M.; Gorjinezhad, S.; Unluevcek, H. S.; Hopke, P. K., Review of factors
509 impacting emission/concentration of cooking generated particulate matter. *Science of The Total*
510 *Environment* **2017,** *586*, 1046-1056.
511 (40) Jimenez, J. L.; Jayne, J. T.; Shi, Q.; Kolb, C. E.; Worsnop, D. R.; Yourshaw, I.; Seinfeld, J. H.;
512 Flagan, R. C.; Zhang, X.; Smith, K. A., Ambient aerosol sampling using the aerodyne aerosol mass
513 spectrometer. *Journal of Geophysical Research: Atmospheres (1984–2012)* **2003,** *108*, (D7).
514 (41) Allan, J. D.; Delia, A. E.; Coe, H.; Bower, K. N.; Alfarra, M. R.; Jimenez, J. L.; Middlebrook, A. M.;
515 Drewnick, F.; Onasch, T. B.; Canagaratna, M. R.; Jayne, J. T.; Worsnop, D. R., A generalised method
516 for the extraction of chemically resolved mass spectra from aerodyne aerosol mass spectrometer
517 data. *J Aerosol Sci* **2004,** *35*, (7), 909-922.
518 (42) Huffman, J. A.; Jayne, J. T.; Drewnick, F.; Aiken, A. C.; Onasch, T.; Worsnop, D. R.; Jimenez, J. L.,
519 Design, Modeling, Optimization, and Experimental Tests of a Particle Beam Width Probe for the
520 Aerodyne Aerosol Mass Spectrometer. *Aerosol Science and Technology* **2005,** *39*, (12), 1143-1163.
521 (43) Middlebrook, A. M.; Bahreini, R.; Jimenez, J. L.; Canagaratna, M. R., Evaluation of Composition-
522 Dependent Collection Efficiencies for the Aerodyne Aerosol Mass Spectrometer using Field Data.
523 *Aerosol Science and Technology* **2012,** *46*, (3), 258-271.
524 (44) Matthew, B. M.; Middlebrook, A. M.; Onasch, T. B., Collection Efficiencies in an Aerodyne
525 Aerosol Mass Spectrometer as a Function of Particle Phase for Laboratory Generated Aerosols.
526 *Aerosol Science and Technology* **2008,** *42*, (11), 884-898.
527 (45) Hennigan, C. J.; Miracolo, M. A.; Engelhart, G. J.; May, A. A.; Presto, A. A.; Lee, T.; Sullivan, A. P.;
528 McMeeking, G. R.; Coe, H.; Wold, C. E.; Hao, W. M.; Gilman, J. B.; Kuster, W. C.; de Gouw, J.;
529 Schichtel, B. A.; Collett Jr, J. L.; Kreidenweis, S. M.; Robinson, A. L., Chemical and physical
530 transformations of organic aerosol from the photo-oxidation of open biomass burning emissions in
531 an environmental chamber. *Atmos. Chem. Phys.* **2011,** *11*, (15), 7669-7686.
532 (46) Aiken, A. C.; DeCarlo, P. F.; Jimenez, J. L., Elemental analysis of organic species with electron
533 ionization high-resolution mass spectrometry. *Anal Chem* **2007,** *79*, (21), 8350-8358.
534 (47) Canagaratna, M. R.; Jimenez, J. L.; Kroll, J. H.; Chen, Q.; Kessler, S. H.; Massoli, P.; Hildebrandt
535 Ruiz, L.; Fortner, E.; Williams, L. R.; Wilson, K. R.; Surratt, J. D.; Donahue, N. M.; Jayne, J. T.; Worsnop,
536 D. R., Elemental ratio measurements of organic compounds using aerosol mass spectrometry:
537 characterization, improved calibration, and implications. *Atmos Chem Phys* **2015,** *15*, (1), 253-272.
538 (48) Noureddini, H.; Teoh, B. C.; Davis Clements, L., Densities of vegetable oils and fatty acids.
539 *Journal of the American Oil Chemists Society* **1992,** *69*, (12), 1184-1188.
540 (49) Lee, B. H.; Lopez-Hilfiker, F. D.; Mohr, C.; Kurtén, T.; Worsnop, D. R.; Thornton, J. A., An Iodide-
541 Adduct High-Resolution Time-of-Flight Chemical-Ionization Mass Spectrometer: Application to
542 Atmospheric Inorganic and Organic Compounds. *Environmental Science & Technology* **2014,** *48*, (11),
543 6309-6317.

(50) Lopez-Hilfiker, F. D.; Mohr, C.; Ehn, M.; Rubach, F.; Kleist, E.; Wildt, J.; Mentel, T. F.; Lutz, A.; Hallquist, M.; Worsnop, D.; Thornton, J. A., A novel method for online analysis of gas and particle composition: description and evaluation of a Filter Inlet for Gases and AEROsols (FIGAERO). *Atmos. Meas. Tech.* **2014,** *7*, (4), 983-1001.
(51) Gong, J. X., Clarifying the standard deviational ellipse. *Geogr. Anal.* **2002,** *34*, (2), 155-167.
(52) Kroll, J. H.; Donahue, N. M.; Jimenez, J. L.; Kessler, S. H.; Canagaratna, M. R.; Wilson, K. R.; Altieri, K. E.; Mazzoleni, L. R.; Wozniak, A. S.; Bluhm, H.; Mysak, E. R.; Smith, J. D.; Kolb, C. E.; Worsnop, D. R., Carbon oxidation state as a metric for describing the chemistry of atmospheric organic aerosol. *Nature Chemistry* **2011,** *3*, (2), 133-139.
(53) Ng, N.; Canagaratna, M.; Jimenez, J.; Chhabra, P.; Seinfeld, J.; Worsnop, D., Changes in organic aerosol composition with aging inferred from aerosol mass spectra. *Atmos Chem Phys* **2011,** *11*, (13), 6465-6474.
(54) Hayes, P. L.; Ortega, A. M.; Cubison, M. J.; Froyd, K. D.; Zhao, Y.; Cliff, S. S.; Hu, W. W.; Toohey, D. W.; Flynn, J. H.; Lefer, B. L.; Grossberg, N.; Alvarez, S.; Rappenglück, B.; Taylor, J. W.; Allan, J. D.; Holloway, J. S.; Gilman, J. B.; Kuster, W. C.; de Gouw, J. A.; Massoli, P.; Zhang, X.; Liu, J.; Weber, R. J.; Corrigan, A. L.; Russell, L. M.; Isaacman, G.; Worton, D. R.; Kreisberg, N. M.; Goldstein, A. H.; Thalman, R.; Waxman, E. M.; Volkamer, R.; Lin, Y. H.; Surratt, J. D.; Kleindienst, T. E.; Offenberg, J. H.; Dusanter, S.; Griffith, S.; Stevens, P. S.; Brioude, J.; Angevine, W. M.; Jimenez, J. L., Organic aerosol composition and sources in Pasadena, California, during the 2010 CalNex campaign. *Journal of Geophysical Research: Atmospheres* **2013,** *118*, (16), 9233-9257.
(55) Lee, A. K. Y.; Willis, M. D.; Healy, R. M.; Onasch, T. B.; Abbatt, J. P. D., Mixing state of carbonaceous aerosol in an urban environment: single particle characterization using the soot particle aerosol mass spectrometer (SP-AMS). *Atmos. Chem. Phys.* **2015,** *15*, (4), 1823-1841.
(56) Aiken, A. C.; Decarlo, P. F.; Kroll, J. H.; Worsnop, D. R.; Huffman, J. A.; Docherty, K. S.; Ulbrich, I. M.; Mohr, C.; Kimmel, J. R.; Sueper, D.; Sun, Y.; Zhang, Q.; Trimborn, A.; Northway, M.; Ziemann, P. J.; Canagaratna, M. R.; Onasch, T. B.; Alfarra, M. R.; Prevot, A. S. H.; Dommen, J.; Duplissy, J.; Metzger, A.; Baltensperger, U.; Jimenez, J. L., O/C and OM/OC ratios of primary, secondary, and ambient organic aerosols with high-resolution time-of-flight aerosol mass spectrometry. *Environmental Science & Technology* **2008,** *42*, (12), 4478-4485.
(57) Schmale, J.; Schneider, J.; Nemitz, E.; Tang, Y. S.; Dragosits, U.; Blackall, T. D.; Trathan, P. N.; Phillips, G. J.; Sutton, M.; Braban, C. F., Sub-Antarctic marine aerosol: dominant contributions from biogenic sources. *Atmos. Chem. Phys.* **2013,** *13*, (17), 8669-8694.
(58) Donahue, N. M.; Epstein, S. A.; Pandis, S. N.; Robinson, A. L., A two-dimensional volatility basis set: 1. organic-aerosol mixing thermodynamics. *Atmos Chem Phys* **2011,** *11*, (7), 3303-3318.
(59) Alfarra, M. R.; Prevot, A. S. H.; Szidat, S.; Sandradewi, J.; Weimer, S.; Lanz, V. A.; Schreiber, D.; Mohr, M.; Baltensperger, U., Identification of the mass spectral signature of organic aerosols from wood burning emissions. *Environmental Science & Technology* **2007,** *41*, (16), 5770-5777.
(60) Lopez-Hilfiker, F. D.; Mohr, C.; Ehn, M.; Rubach, F.; Kleist, E.; Wildt, J.; Mentel, T. F.; Carrasquillo, A. J.; Daumit, K. E.; Hunter, J. F.; Kroll, J. H.; Worsnop, D. R.; Thornton, J. A., Phase partitioning and volatility of secondary organic aerosol components formed from alpha-pinene ozonolysis and OH oxidation: the importance of accretion products and other low volatility compounds. *Atmos Chem Phys* **2015,** *15*, (14), 7765-7776.
(61) Yatavelli, R. L. N.; Mohr, C.; Stark, H.; Day, D. A.; Thompson, S. L.; Lopez-Hilfiker, F. D.; Campuzano-Jost, P.; Palm, B. B.; Vogel, A. L.; Hoffmann, T.; Heikkinen, L.; Aijala, M.; Ng, N. L.; Kimmel, J. R.; Canagaratna, M. R.; Ehn, M.; Junninen, H.; Cubison, M. J.; Petaja, T.; Kulmala, M.; Jayne, J. T.; Worsnop, D. R.; Jimenez, J. L., Estimating the contribution of organic acids to northern hemispheric continental organic aerosol. *Geophys Res Lett* **2015,** *42*, (14), 6084-6090.
(62) Stark, H.; Yatavelli, R. L. N.; Thompson, S. L.; Kang, H.; Krechmer, J. E.; Kimmel, J. R.; Palm, B. B.; Hu, W.; Hayes, P. L.; Day, D. A.; Campuzano-Jost, P.; Canagaratna, M. R.; Jayne, J. T.; Worsnop, D. R.; Jimenez, J. L., Impact of Thermal Decomposition on Thermal Desorption Instruments: Advantage of

Thermogram Analysis for Quantifying Volatility Distributions of Organic Species. *Environmental Science & Technology* **2017,** *51*, (15), 8491-8500.
(63) Coggon, M. M.; Veres, P. R.; Yuan, B.; Koss, A.; Warneke, C.; Gilman, J. B.; Lerner, B. M.; Peischl, J.; Aikin, K. C.; Stockwell, C. E.; Hatch, L. E.; Ryerson, T. B.; Roberts, J. M.; Yokelson, R. J.; de Gouw, J. A., Emissions of nitrogen-containing organic compounds from the burning of herbaceous and arboraceous biomass: Fuel composition dependence and the variability of commonly used nitrile tracers. *Geophys Res Lett* **2016,** *43*, (18), 9903-9912.
(64) Brady, J. M.; Crisp, T. A.; Collier, S.; Kuwayama, T.; Forestieri, S. D.; Perraud, V.; Zhang, Q.; Kleeman, M. J.; Cappa, C. D.; Bertram, T. H., Real-Time Emission Factor Measurements of Isocyanic Acid from Light Duty Gasoline Vehicles. *Environmental Science & Technology* **2014,** *48*, (19), 11405-11412.
(65) Roberts, J. M.; Veres, P. R.; Cochran, A. K.; Warneke, C.; Burling, I. R.; Yokelson, R. J.; Lerner, B.; Gilman, J. B.; Kuster, W. C.; Fall, R.; de Gouw, J., Isocyanic acid in the atmosphere and its possible link to smoke-related health effects (vol 108, pg 8966, 2011). *Proceedings of the National Academy of Sciences of the United States of America* **2011,** *108*, (41), 17234-17234.
(66) Huang, Q.; Wang, L.; Han, S., The genotoxicity of substituted nitrobenzenes and the quantitative structure-activity relationship studies. *Chemosphere* **1995,** *30*, (5), 915-923.
(67) Sakhno, L. O., Variability in the fatty acid composition of rapeseed oil: Classical breeding and biotechnology. *Cytology and Genetics* **2010,** *44*, (6), 389-397.
(68) Orsavova, J.; Misurcova, L.; Ambrozova, J.; Vicha, R.; Mlcek, J., Fatty Acids Composition of Vegetable Oils and Its Contribution to Dietary Energy Intake and Dependence of Cardiovascular Mortality on Dietary Intake of Fatty Acids. *International Journal of Molecular Sciences* **2015,** *16*, (6), 12871.
(69) Reyes-Villegas, E.; Priestley, M.; Ting, Y. C.; Haslett, S.; Bannan, T.; Le breton, M.; Williams, P. I.; Bacak, A.; Flynn, M. J.; Coe, H.; Percival, C.; Allan, J. D., Simultaneous Aerosol Mass Spectrometry and Chemical Ionisation Mass Spectrometry measurements during a biomass burning event in the UK: Insights into nitrate chemistry. *Atmos. Chem. Phys. Discuss.* **2017,** *2017*, 1-22.
(70) Chow, J. C.; Watson, J. G.; Lowenthal, D. H.; Chen, L. W. A.; Zielinska, B.; Mazzoleni, L. R.; Magliano, K. L., Evaluation of organic markers for chemical mass balance source apportionment at the Fresno Supersite. *Atmos. Chem. Phys.* **2007,** *7*, (7), 1741-1754.
(71) Pei, B.; Cui, H. Y.; Liu, H.; Yan, N. Q., Chemical characteristics of fine particulate matter emitted from commercial cooking. *Front Env Sci Eng* **2016,** *10*, (3), 559-568.

Table 1. List of all cooking experiments.

	Food	Exp. #	Diluted	OA [µg.m^{-3}]	SMPS [µg.m^{-3}]	Diameter (nm)	Peak dM/DlogDp	Filter #
Deep fried	Fish&chips	E1	N	23.8	16.1	346	37	F0
	Fish&chips	E2	N	54.7	21.9	429	18	F1
	Fish&chips	E3	Y	5.3	4.3	385	10	F2
	Fish&chips	E4	Y	5.8	4.3	334	11	
	Burgers	E5	Y	10.8	13.2	98	28	F3
	Burgers	E6	N	**	**	**	**	F4
	Burgers	E7	N	**	**	**	**	F5
	Burgers	E8	N	87.9	**	**	**	F6
	Burgers	E9	N	93.7	**	**	**	
	Burgers	E10	Y	7.6	11.1	136	17	F7
	Burgers	E11	Y	9.1	21.5	131	47	
	Sausages	E12	Y	9.7	12.3	105	18	F8
	Sausages	E13	N	183.0	223.5	151	452	F9
Shallow fried	Tomato	E14	N	240.1	226.5	346	286	F10
	Mushroom	E15	N	112.7	117.9	334	204	
	Eggs	E16	N	28.0	47.0	102	65	
	Bacon	E17	N	219.7	247.6	157	392	
	Black puddin	E18	N	19.0	9.6	146	12	
	Sausages	E19	N	424.1	395.0	260	540	
	Tomato	E20	Y	15.3	17.7	209	34	F11
	Mushroom	E21	Y	10.8	7.5	241	12	
	Eggs	E22	Y	1.8	**	**	**	
	Bacon	E23	Y	4.6	**	**	**	
	Sausages	E24	Y	16.8	**	**	**	
	Black puddin	E25	Y	4.0	3.5	109	5	
	Bacon	E26	Y	2.9	2.8	64	4	
	Salmon	E27	Y	20.8	18.2	131	30	F12
	Salmon_SF	E28	Y	16.9	16.1	131	32	
	Burgers	E29	Y	30.9	23.2	131	48	F13
	Vegetables_SF	E30	Y	61.1	**	**	**	F14
	Vegetables_SF	E31	Y	96.1	45.3	399	69	
	Pork	E32	Y	21.3	22.3	122	37	F15
	Lamb	E33	Y	49.0	51.8	175	98	F16
	Lamb_SF	E34	Y	8.3	8.3	269	13	
	Chicken	E35	Y	26.8	33.3	118	58	F17
	Chicken_SF	E36	Y	8.0	8.7	98	14	

E= Experiment, N=No Y=Yes, SF = steer-fried, ** samples were lost. , F=Filter.

642

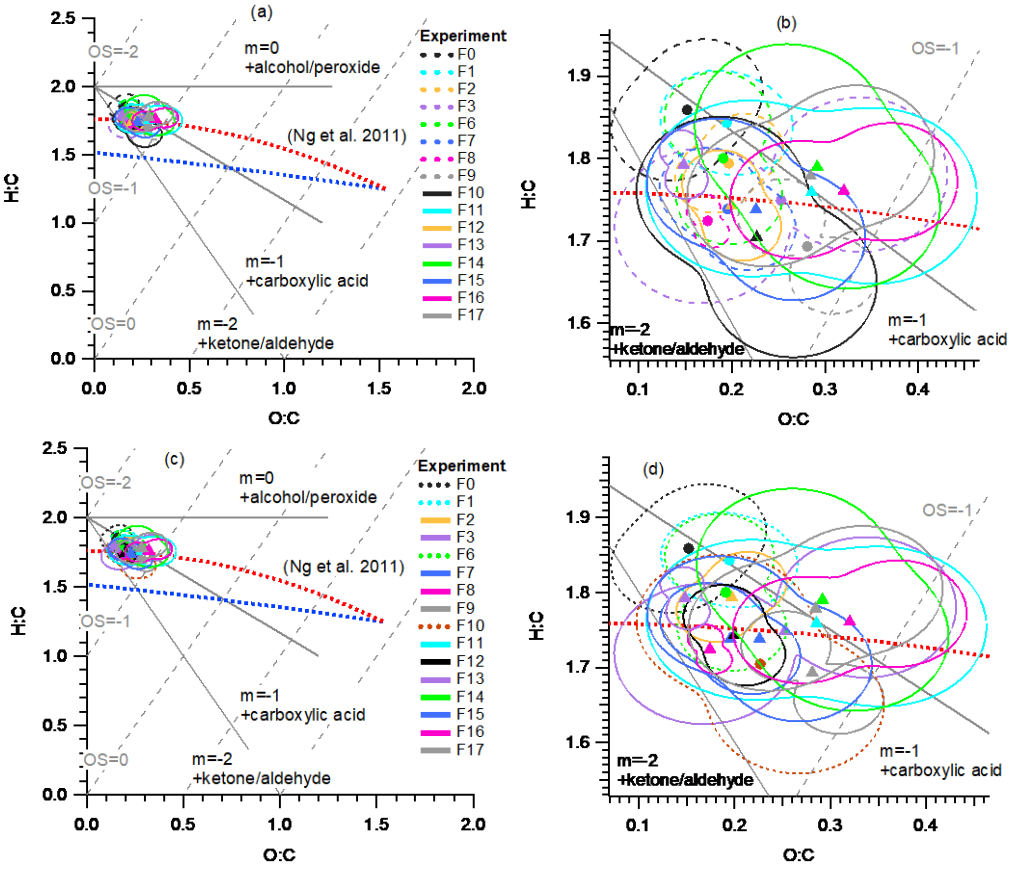

643

644 **Figure 1.** Van Krevelen diagram with mean (markers) and SDE (lines) of O:C and H:C.

645

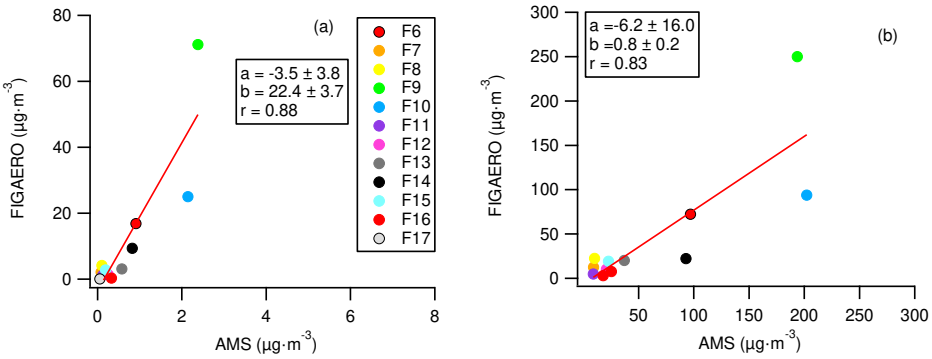

646

647 **Figure 2.** FIGAERO-AMS comparison for levoglucosan (a) and OA (b) concentrations. Red

648 lines show linear regression. Description of filter numbers (F0-F17) is provided in Table 1.

649

650

Table 2. Cooking markers in the gas phase.

Formula	Name	*	F6	F7	F8	F9	F10	F11	F12	F13	F14	F15	F16	F17	Mass + I
CHNO	Isocyanic acid	G	7.84	17.01	13.11	3.94	9.16	1.56		3.34	2.14	1.32	2.68		169.91
		P													
		R													
CH_2O_2	Formic acid	G	16558.40	13439.20	8726.79	14167.10	5146.27		762.00						172.91
		P		1.12	2.40	2.18							0.11		
		R		65.38	40.60	83.42									
$C_3H_4O_2$	Acrylic acid	G	5167.44	1351.57	623.29	2737.11	55.43	8.42	12.65	25.36	19.44	1.97	3.99	13.57	198.93
		P	0.02	0.01	0.01	0.25									
		R	1404.82	766.57	467.14	143.03									
$C_3H_6O_2$	Propionic acid	G	17.58	9.24	4.57	8.63	6.02	3.66	1.54	5.62	6.17	0.89	1.94	1.42	200.95
		P	0.01			0.02									
		R	9.33			4.55									
$C_3H_6O_3$	Hydroxypropionic	G	109170.00	79445.60	78302.60	108587.00	3672.54		7397.47	5085.04		12600.70	11146.40	6038.39	216.94
		P	31.60	37.33	42.43	83.59	11.40	0.93	4.43	7.40	1.59	21.32	3.32	1.81	
		R	17.20	11.55	20.58	16.68	1.07		7.88	7.94		7.58	15.16	9.51	
$C_3H_4O_4$	Malonic Acid	G	215.06	184.02	149.88	198.71	5.73								230.92
		P	0.25	0.15	0.20	0.76	0.04								
		R	4.26	6.75	8.38	3.37	0.42								
$C_6H_{10}O_2$	Hexanoic acid	G	109.34	145.26	109.86	72.45	20.85	7.58	4.52	7.87	12.41				240.97
		P	0.11	0.04	0.07	0.46	0.19	0.01	0.03	0.01	0.004	0.06	0.06	0.03	
		R	4.83	19.22	17.52	2.01	0.36	1.16	0.70	8.89	16.08				
$C_6H_{10}O_4$	Adipic acid	G	99.32	105.15	95.84	144.49	15.05								272.96
		P	0.36			2.27	0.56								
		R	1.37			0.82	0.09								

* G= Gas [formic equiv. ppt], P = Particle [formic equiv. $\mu g \cdot m^{-3}$], R= G/P Ratio [calculated using raw signal]. Mass+I = Molecular mass of compound + I. Description of filters (f0-f17) is provided in Table 1.

Table 3. Cooking markers in the particle phase.

Formula	Name	*	F6	F7	F8	F9	F10	F11	F12	F13	F14	F15	F16	F17	Mass + I
$C_4H_6O_4$	Succinic acid	G	431.33	500.52	275.54	855.15	73.22	2.42							244.93
		P	14.05	0.93	2.00	53.14	6.61	0.08	0.15	0.38	0.97				
		R	0.15	2.92	1.54	0.21	0.04	0.04							
$C_5H_8O_4$	Glutaric acid	G	174.82	226.38	246.82	255.09	83.62	113.96	50.31	49.86	70.40	44.02			258.94
		P	4.12	0.51	1.13	28.63	10.83	0.33	0.45	1.01	2.37	0.80	0.11	0.04	
		R	0.21	2.43	2.44	0.11	0.03	0.43	0.53	0.57	0.16	0.70			
$C_7H_{12}O_4$	Pimelic acid	G	51.36	62.47	81.97	86.45	43.75	21.60		0.67	9.52				286.98
		P	0.99	0.20	0.38	4.70	1.37	0.05	0.07	0.15	0.36	0.02	0.05	0.04	
		R	0.26	1.73	2.44	0.24	0.11	0.55		0.05	0.14				
$C_6H_{10}O_5$	Levoglucosan	G	679.57	762.16	925.19	1351.71	427.93	261.77	76.61	117.53	521.84	165.73			288.96
		P	16.83	2.09	4.16	71.14	25.00	1.18	1.28	3.10	9.37	2.77	0.28	0.06	
		R	0.20	1.98	2.48	0.24	0.06	0.28	0.28	0.44	0.29	0.77			
$C_8H_{14}O_4$	Suberic acid	G	3.26	8.86	9.40	5.50	6.59	7.64							300.99
		P	0.29	0.06	0.12	1.06	0.95	0.05	0.10	0.16	0.20	0.06	0.07	0.05	
		R	0.06	0.83	0.85	0.07	0.02	0.20							
$C_9H_{16}O_4$	Azelaic acid	G		2.93	1.25			4.97					8.24	0.55	315.01
		P	0.37	0.07	0.16	1.24	0.70	0.04	0.10	0.20	0.12	0.07	0.11	0.06	
		R		0.22	0.09			0.14					0.34	0.02	
$C_{10}H_{18}O_4$	Sebacic acid	G						12.71	4.97	7.34	9.44	0.53	41.15	23.65	329.03
		P	0.08	0.04	0.09	0.32	0.34	0.02	0.06	0.14	0.06	0.03	0.18	0.09	
		R						0.67	0.37	0.62	0.78	0.25	1.02	0.78	
$C_{12}H_{22}O_4$	Dodecanedioic	G													357.06
		P	0.02			0.07	0.16	0.01	0.02	0.04	0.02		0.02	0.01	
		R													
$C_{16}H_{32}O_2$	Palmitic acid	G						36.36	19.19	23.19	19.12	12.96	0.06		383.14
		P	0.79	0.43	0.76	1.73	0.84	0.14	0.54	1.10	0.23	0.49	0.31	0.06	
		R						0.33	0.17	0.24	0.44	0.34	0.00		
$C_{17}H_{34}O_2$	Margaric acid	G						1.40	0.53	1.06	0.83	0.76			397.16
		P	0.06	0.03	0.07	0.13	0.09	0.02	0.04	0.12	0.04	0.05	0.06	0.01	
		R						0.12	0.06	0.10	0.12	0.20			
$C_{18}H_{32}O_2$	Linoleic acid	G		6.94	3.80			40.76	29.16	32.13	28.49	25.28	5.68	4.72	407.14
		P	1.44	0.59	0.91	2.82	1.96	0.28	0.66	1.27	0.50	0.92	0.18	0.12	
		R		0.06	0.05			0.18	0.21	0.29	0.30	0.35	0.15	0.11	
$C_{18}H_{34}O_2$	Oleic acid	G		9.90	2.47			77.77	56.31	65.38	61.71	55.90	9.54	9.88	409.16
		P	4.27	1.88	2.92	8.54	3.94	0.61	1.49	3.85	1.36	2.15	0.93	0.37	
		R		0.03	0.01			0.16	0.18	0.20	0.24	0.33	0.05	0.08	

* G= Gas [formic equiv. ppt], P = Particle [formic equiv. $\mu g \cdot m^{-3}$], R= G/P Ratio (of raw signals). Mass+I = Molecular mass of compound + I. Description of filters (f0-f17) is provided in Table 1.

TOC art